International Journal of Nanoelectronics and Materials

In Press, Accepted Manuscript – Note to user

Correlation between crystal structure and thermal reaction of TiO_2 - Graphene Oxide

S. K. Kamarudin, M. A. Idris[1,2]*, N. F. M. Yunos[1,2], J. Banjuraizah[1], L. N. Ho[1,2], S. N. Sabki[3] and S. Illias[4]

[1] Faculty of Chemical Engineering Technology, Universiti Malaysia Perlis (UniMAP), Perlis, Malaysia.
[2] Frontier Materials Research, Centre of Excellence (FrontMate), Universiti Malaysia Perlis (UniMAP), Perlis, Malaysia.
[3] Faculty of Electronic Engineering Technology, Universiti Malaysia Perlis (UniMAP), Perlis, Malaysia.
[4] Faculty of Mechanical Engineering Technology, Universiti Malaysia Perlis (UniMAP), Perlis, Malaysia.

Received 19 March 2021, revised 23 March 2020, Accepted 05 April 2021

ABSTRACT

TiO_2 - Graphene oxide (GO) (GO = 0-1.0wt %) powders were synthesized using sol-gel method and annealed at 500°C. The samples were then characterized using X-ray diffraction (XRD). The additional of GO gave significant influence on the crystal structure of TiO_2. The lattice parameter of TiO_2 were increased with decreasing GO concentration. The unit cell volume of TiO_2-GO annealed in N_2 decreased with the oxygen occupancy. In contrary, the TiO_2-GO annealed in O_2 has an increase in O_2 occupancies in the lattice that was nearly proportional to its unit cell volume. A continuous weight loss was recorded by TGA at a temperature range of T= 30 - 1000°C that were associated with H2O, C-H and C-O species. It is concluded that the Ti-O-C and Ti-C bonds were formed for samples annealed in O_2 and N_2 respectively. The weight loss of TiO_2-GO annealed in O_2 is lesser than that annealed in N_2 for same concentration additional GO into TiO_2.

Keywords: TiO_2, Carbon Addition, Graphene Oxide

1. INTRODUCTION

Photocatalytic reaction needs a well-engineered material to facilitate a range of solar energy conversion processes. This is including splitting of water, self-cleaning surface and power generation. Metal oxide is a promising candidate as the best photocatalytic oxide due to its chemical stability. However, the band gap of metal oxide is relatively bigger that it is unable to be activated by visible light. Thus, additional extrinsic species were mixed together with the metal oxide to lower its band gap. Such species additional process is important to include the understanding of electronic and ionic balance between extrinsic and intrinsic species. This is because the species could shift the stoichiometric to nonstoichiometric state of the metal oxide that possibly improve its photocatalytic properties [1–3].

TiO_2 is one of the nonstoichiometric compounds that had been intensively studied by many researchers as it is promising in many scientific applications including photocatalytic activity [1–5]. The nonstoichiometry in TiO_2 is controlled by the atomic defects including oxygen vacancies, substitutional and interstitial defects at the host lattice. It had been reported that the properties of TiO_2 is strongly influenced by its defect disorder [2,6]. The intensive study on aliovallent species of dopant effects on defect disorder had been reported by Janusz et al. [6–10], whereas they have successfully derived the equilibrium constant of TiO_2.

*Email : asri@unimap.edu.my

The formation of defects in TiO_2 may be represented using Kröger-Vink notation by the following defect equilibria [6]:

$$O_O \leftarrow V_O^{\cdot\cdot} + 2e' + \frac{1}{2}O_2 \quad (1)$$

$$2O_O + Ti_{Ti} \leftarrow Ti_i^{\cdot\cdot\cdot} + 3e' + O_2 \quad (2)$$

$$2O_O + Ti_{Ti} \leftarrow Ti_i^{\cdot\cdot\cdot\cdot} + 4e' + O_2 \quad (3)$$

$$nil \leftarrow e' + h^{\cdot} \quad (4)$$

This could be understood that the defect disorder in TiO_2 is controlled by atomic defects including oxygen vacancies, substitutional and interstitial defects at the host lattice. However, in application such as photocatalytic, it is demanded that the spontaneous recombination of electron and electron hole that is shown in eq. (4) could be avoided at atomic lattice [11–14]. It is reported that the recombination could be achieved by introducing C species [11,12,15–17]. However, the explanation of the reaction of C and TiO_2 are scarcely found even though there is a few theoretical study have been reported, showing the possible reaction between these species [16,18–20]. Accordingly, the doping of C species including graphene [11–14] needs a further and detailed study especially on its defects and other reaction within TiO_2 and C species.

It is reported that the C content will enhance the photocatalytic activity [21–26]. However, the enhancement will become diminution after having a maximum photocatalytic activity at a certain carbon content. Carbon poisoning affected the most of electrochemical devices [27]. It is reported that the main issues occurred when the carbon that existed in the lattice lead to performance reduction due to the formation of metal carbonate on the metal oxide. The formation of the metal carbonate may vary based on the metal oxide matrix and is supposed to be in the range of 500 – 600 ℃. Teruhisa et al. reported that the carbonate is formed until 1.5 nm depth on the surface of TiO_2 that was annealed at 400 and 500 ℃ [28]. Thus, the study of C mixed in metal oxide matrix still needs to face a long list of obstacles that mainly focused on Ti–O–C reaction.

The aim of the present work is to assess the incorporation of C anions into the TiO_2 lattice. Graphene oxide was intentionally added at the concentration of 0 – 1.0 wt% as a C dopant and annealed at 500°C in different oxygen partial pressure. Different concentration of GO was added to investigate the effect of carbon from the GO on the crystal structure. The structural properties of the samples in the form of powder were characterized using X-ray diffraction (XRD). Next, the crystal structure will be correlated to its thermal kinetic by thermogravimetric and differential thermal analysis (TGA-DTA).

2. MATERIAL AND METHODS

2.1 Sample Preparation.

TiO_2 was synthesized using sol–gel method by the hydrolysis of titanium isopropoxide ($Ti(OC_4H_9)_4$, Sigma Aldrich 99.99%). 6.4mL Titanium isopropoxide was added and stirred into the mixture solution of 18.6 mL of isoprophyl alcohol. Followed by an addition of 10.6mL acetic acid (HmBG 98.00%). Then, GO powder was mixed into the solution according to the weight fraction range of 0.2%– 1.0%. Finally, a 3-5 drops of deionized water were added into the solution while stirring. After stirring for 24 h, the solution became gel and was dried in an oven at 80 °C for 24 h to form powder annealed at 500°C for 6 h. Further annealing was done for all samples in N_2 and O_2 atmosphere at 500°C.

2.2 Characterizations.

XRD patterns were obtained with Shidmadzu XRD 6000 2500V using Cu Ka radiation. Thermogravimetry and differential thermal analysis (TG-DTA) were recorded in N_2 and O_2 atmosphere by using TG-DTA system (METTLER TOLEDO, Model TGADSC1).

3. RESULTS AND DISCUSSION

Phase and structure of the samples were investigated by XRD where it is shown in Figure 1 for different weight percentage of GO. All peaks observed indicated anatase structure of titanium dioxide according to ICSD pattern 98-001-7818 (anatase). Obviously, all of the peak width increased with the increment of the GO content in TiO_2 bulk. It is also can be seen that the XRD peak of (105) and (211) crystal plane is overlapping with each other at GO content of 0.6 and 1.0wt%. This shows that the partial crystal changes occurred with the increment of GO content that needed an allocation of carbon species into TiO_2 lattice. Li et al. [29] reported that the shifted XRD peak diffraction at 23°–27° indicates the carbon incorporation into the anatase crystals. However, there is no shifting shown in Figure 1. Hence, the results by Li et al. may be influenced by other factor including instrumental causes and internal effects of sample. The latter could be argued, if it is dedicated to the incorporation of C based on the results by Li et al. that shows the increased of C with no further peak shift. Therefore, XRD alone could not be the ultimate tool to be used in confirming the C incorporation in the TiO_2 matrix. Other reports [30–32] are in agreement with our results in Figure 1.

Further refinement of the XRD pattern was performed by Rietveld method where high reliability index less than 12 was attained (R<12). The O-2 occupancy factor is estimated through the Reitveld refinement and shown in Figure 2 together with the unit cell volume. It is shown that the unit cell volume for the sample annealed in N_2 decreased with the oxygen occupancy. In contrary, the TiO_2 sample that was annealed in O_2 has an increase in O_2 occupancies in the lattice that was nearly proportional to its unit cell volume. Thus, it can be concluded that the changes in the pattern of the unit cell volume and oxygen occupancy is closely related to each other. The highest unit cell volume was attained at the additional of 0.2wt% GO annealed in N_2 which is 136.35 Å.

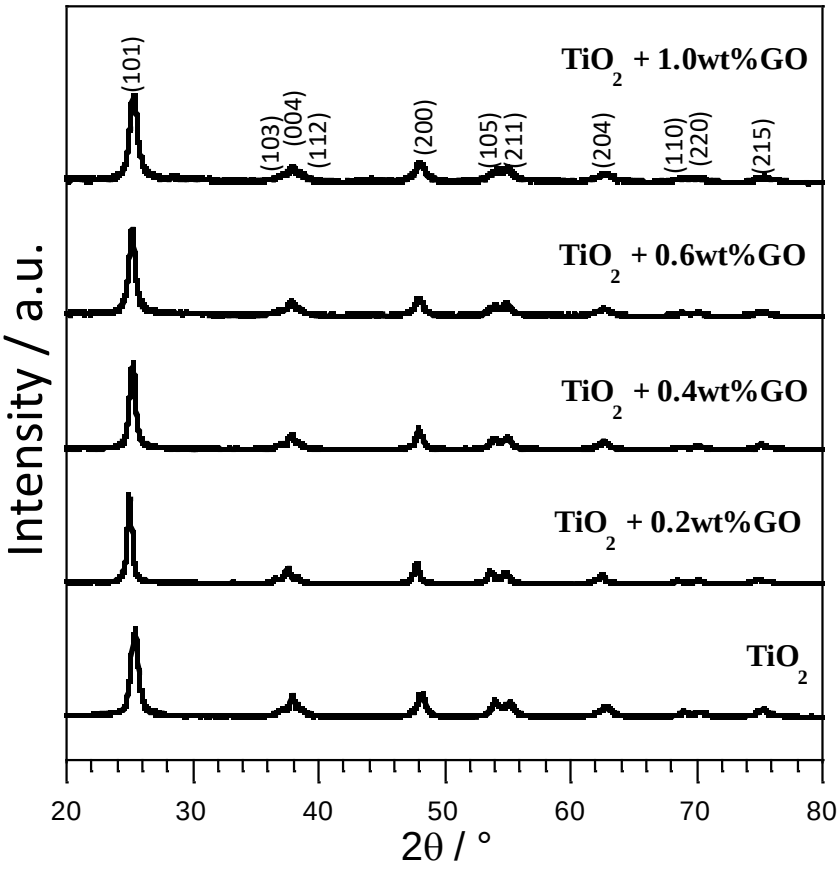

Figure 1. XRD pattern of sample TiO_2, TiO_2 with 0.2wt% GO, TiO_2 with 0.4wt% GO , TiO_2 with 0.6wt% GO and TiO_2 with 1.0wt% GO.

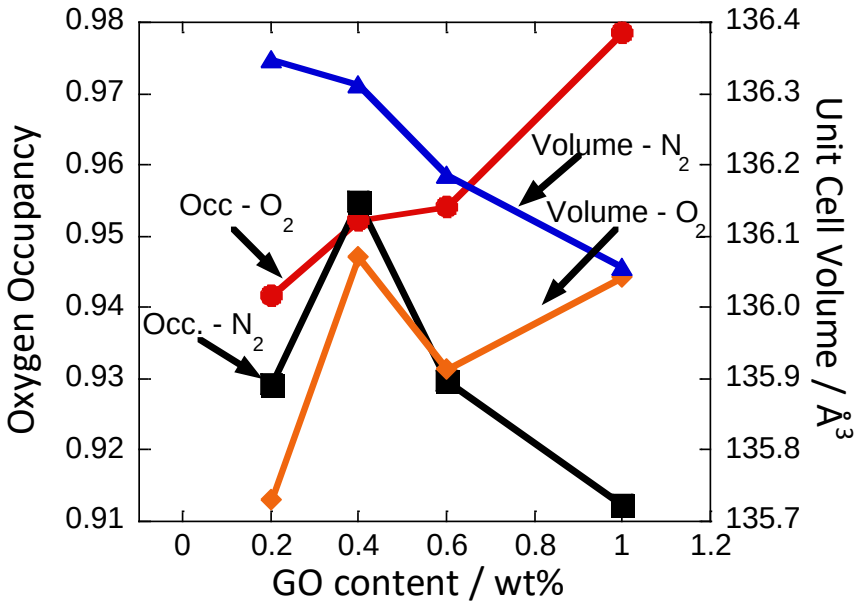

Figure 2. Unit cell volume and oxygen occupancy in TiO_2 lattice within the additional of 0.2 – 1.0wt% of GO.

Figure 3 to Figure 5 show the results of TG-DTA for the samples measured in O_2 and N_2 atmosphere at a temperature range of T= 25 – 1000°C and heating rate of 4.0°C/min. According to the DTA curves in Figure 3 to Figure 5, it is shown that there are several increments and decrements of heat flow which are associated to the exothermic and endothermic reactions, respectively. The exothermic and endothermic reactions are in agreement with the one that were reported by other works [33,34]. Both of the reactions occurred at the same temperature for the concentration of 0.2 – 1.0wt% GO. However, it could be seen that the endothermic reaction at 300°C for the sample annealed in O_2 was shifted to the higher temperature as well as for the samples annealed in N_2 in all concentration of additional GO.

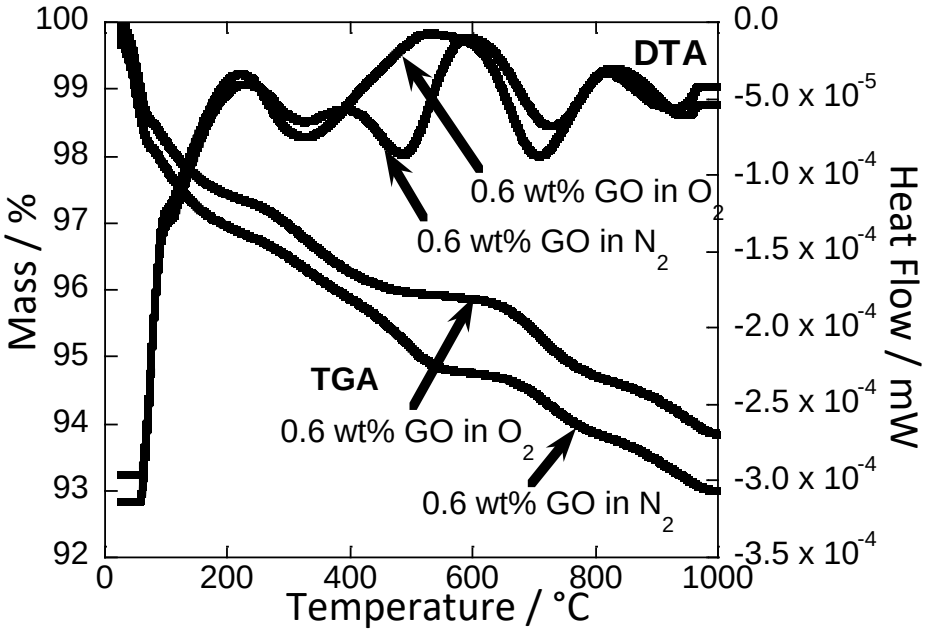

Figure 3. TG-DTA result of TiO_2 with addition of 0.6wt% GO annealed in O_2 and N_2 atmosphere.

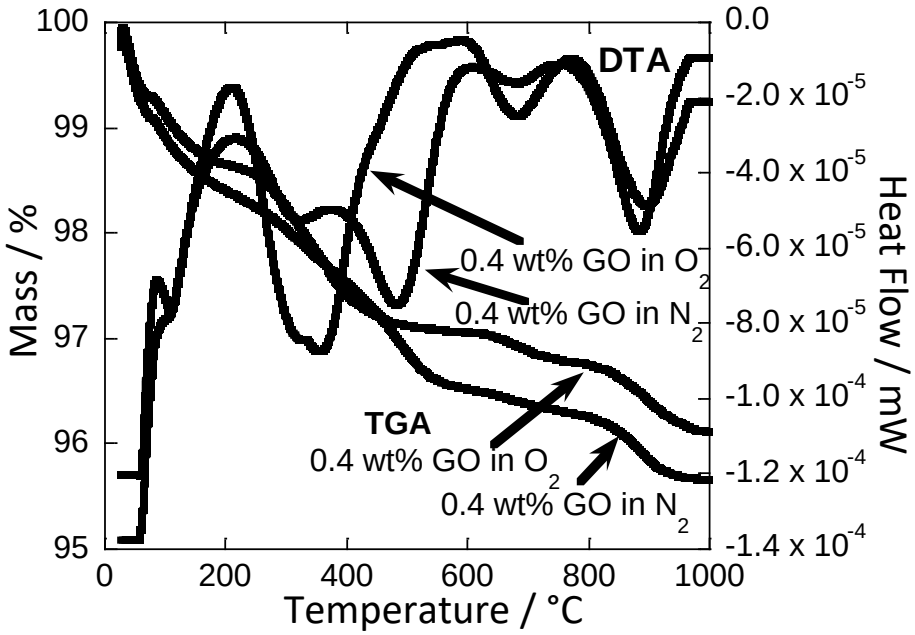

Figure 4. TG-DTA result of TiO_2 with addition of 0.4 wt% GO annealed in O_2 and N_2 atmosphere.

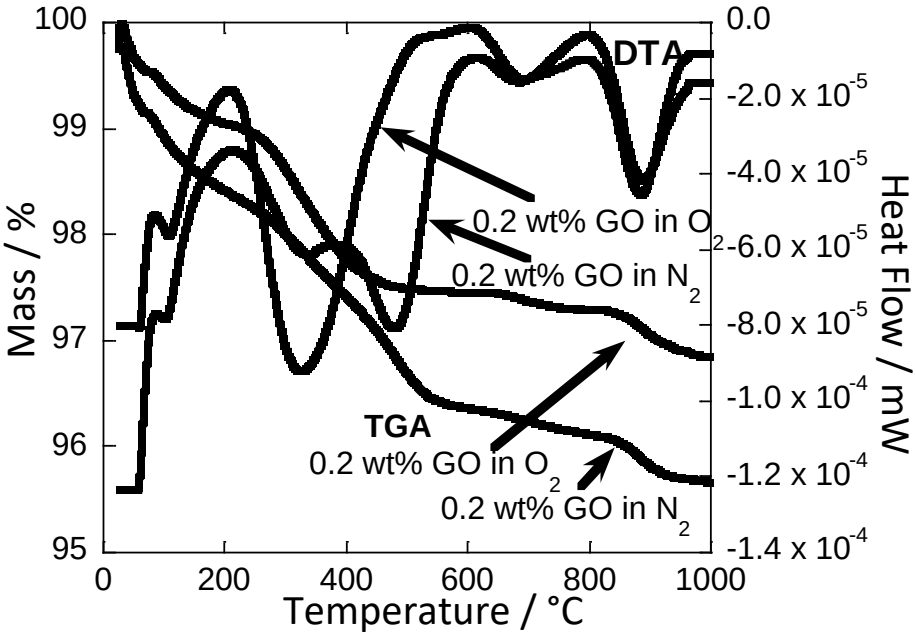

Figure 5. TG-DTA result of TiO_2 with addition of 0.2 wt% GO annealed in O_2 and N_2 atmosphere.

The TGA curves started with a sudden weight loss at room temperature up to about 150°C and continuously decline afterwards until the end of the temperature measurement. This is seen for all curves in Figure 3 to Figure 5. The final mass which was attained at 1000°C indicated that the mass reduction in N_2 is larger than that in O_2 atmosphere. This indicates that the bulk reduction involved more species in the bulk rather than the surface. Dependent on the quality of the C sources, the weight loss could be continued beyond 900°C [32,35,36]. As the weight loss trend is identical with other C sources, this could be concluded that, the weight loss shown by the TGA

results are an effect of the reaction of the C matrix (GO). This conclusion is applied for both annealed samples in N_2 and O_2 atmospheric condition.

It is reported that the reaction of TiO_2 and GO in O_2 at the temperature range of between 400 – 500°C contributes to Ti-O-C bond [14,34,37–39] in the core region. While the reaction in N_2 condition will produce Ti-C bond as a core. Both of these core regions are surrounded by C-H, C=O (hydroxyl carbon) O=C-O (carboxyl carbon) [14,37–40] that associated to carbonate-like species. The metal-oxygen and carbon-oxygen bond is the active region which is could be found in other carbon enhanced photocatalytic materials [41]. It is also reported that other species that existed are C-C (graphitic phase) and Ti-O-Ti bonds. Thus, the continued weight loss in our TGA results (Figure 3 - Figure 5) can be concluded as an effect of carbon bond at the outer region of TiO_2. The trend of the weight loss agreed with most of the literatures [14,37–40]. This carbon bond is reported to be able to form a carbonate [20,30,38,42,43] solution especially at the temperature of about 500 - 600°C.

The correlation of thermal reaction and the crystal was shown in Figure 6. The curves were taking the isothermal measurement at 500°C of TGA data as the weight loss during heating and lattice volume calculated from XRD. The weight loss of TiO_2-GO annealed in O_2 is lesser than that annealed in N_2 for same concentration additional GO into TiO_2. Thus affects the lattice volume of samples in O_2 is becomes smaller than that annealed in N_2. The correlation of both conditions of these isothermal properties to the GO content seems hard to conclude. The difficulty had been highlighted by Valentin et al. [19] in their simulation works that of TiO_2 with the different reaction of C at the low (0.47%) and high (1.41%) doping. The high doping C is more complicated where the C from GO exhibits unexpected stabilization caused by multidoping effects, interpreted as inter-species redox processes [19]. This could introduce an unpredictable change in the crystal lattice. However, the crystal size measurement by Zerjav et al. [17] shows insignificant changes with the increment in GO content. This inconsistency may have resulted from difference oxygen partial pressure, $p(O_2)$ which is the crucial effect in TiO_2 lattice [44,45].

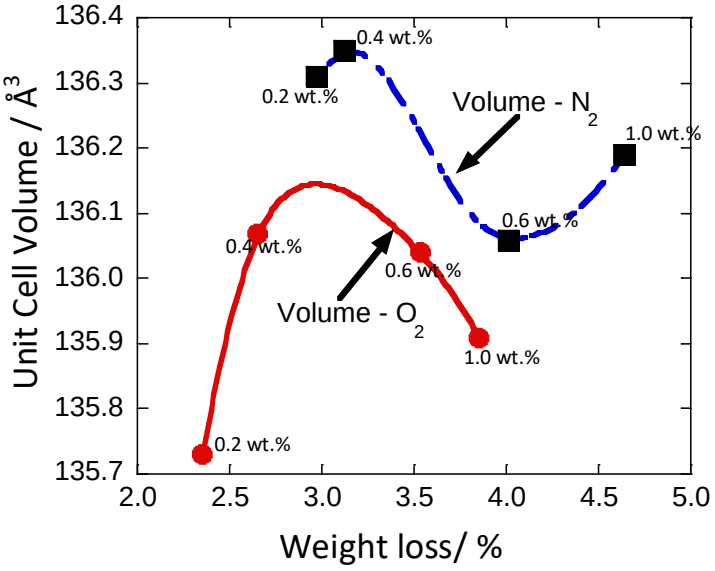

Figure 6. Correlation between unit cell volume and weight loss during thermal reaction of TiO_2 – GO at temperature T = 500°C.

4. CONCLUSION

GO with concentration of 0 – 1.0wt% were successfully added to TiO_2 samples prepared by sol-gel method and annealed at 500°C. All of the annealed samples were confirmed in TiO_2 anatase phase. The largest crystallite was recorded by sample 0.2wt% GO with the size of 136.35 Å. The TGA curves show a sudden weight loss at room temperature up to about 150°C and continuously decline until the end of the temperature measurement that associated with H2O, C-H and C-O species. Base on the TGA results and other reported literatures, it is predicted that Ti-O-C and Ti-C bonds were formed for sample annealed at O_2 and N_2 respectively. The weight loss of TiO_2-GO annealed in O_2 is lesser than that annealed in N_2 for same concentration additional GO into TiO_2. The unit cell volume of TiO_2-GO annealed in N_2 decreased with the oxygen occupancy. In contrary, the TiO_2-GO annealed in O_2 has an increase in O_2 occupancies in the lattice that was nearly proportional to its unit cell volume.

ACKNOWLEDGEMENTS

The author would like to acknowledge the support from the Fundamental Research Grant Scheme (FRGS) under grant number of FRGS/2/2014/SG06/UNIMAP/02/3 and from the Ministry of Higher Education Malaysia. The authors also acknowledge the financial support from Mentorship Research Grants under Research Management and Innovation Center (RMIC), and Faculty of Chemical Engineering Technology, Universiti Malaysia Perlis, (UniMAP) for this research.

REFERENCES

[1] J. Nowotny, Surface re-equilibration kinetics of nonstoichiometric oxides, J. Mater. Sci. 12 (1977). https://doi.org/10.1007/bf02426852.

[2] J. Nowotny, M.A. Alim, T. Bak, M.A. Idris, M. Ionescu, K. Prince, M.Z. Sahdan, K. Sopian, M.A. Mat Teridi, W. Sigmund, Defect chemistry and defect engineering of TiO2-based semiconductors for solar energy conversion, Chem. Soc. Rev. 44 (2015). https://doi.org/10.1039/c4cs00469h.

[3] J. Nowotny, Surface segregation of defects in oxide ceramic materials, Solid State Ionics. 28–30 (1988). https://doi.org/10.1016/0167-2738(88)90363-3.

[4] J. Nowotny, M. Rekas, Defect structure, electrical properties and transport in barium titanate. II. Consistency requirements between defect models and crystal properties, Ceram. Int. 20 (1994). https://doi.org/10.1016/0272-8842(94)90056-6.

[5] P. Kofstad, Nonstoichiometry, diffusion, and electrical conductivity in binary metal oxides, Wiley-Interscience, New York, 1972.

[6] J. Nowotny, T. Bak, M.K. Nowotny, L.R. Sheppard, Defect chemistry and electrical properties of titanium dioxide. 1. Defect diagrams, J. Phys. Chem. C. 112 (2008). https://doi.org/10.1021/jp074565u.

[7] T. Nakajima, L.R. Sheppard, K.E. Prince, J. Nowotny, T. Ogawa, Niobium segregation in TiO2, Adv. Appl. Ceram. 106 (2007). https://doi.org/10.1179/174367607X156034.

[8] L.R. Sheppard, A.J. Atanacio, T. Bak, J. Nowotny, M.K. Nowotny, K.E. Prince, Niobium diffusion in niobium-doped titanium dioxide, J. Solid State Electrochem. 13 (2009). https://doi.org/10.1007/s10008-008-0717-x.

[9] L.R. Sheppard, A.J. Atanacio, T. Bak, J. Nowotny, K.E. Prince, Bulk diffusion of niobium in single-crystal titanium dioxide, J. Phys. Chem. B. 111 (2007). https://doi.org/10.1021/jp0678709.

[10] L.R. Sheppard, A. Atanacio, T. Bak, J. Nowotny, K.E. Prince, Effect of niobium segregation on surface properties of titanium dioxide, in: Sol. Hydrog. Nanotechnol., 2006. https://doi.org/10.1117/12.674547.

[11] J. Yu, T. Ma, S. Liu, Enhanced photocatalytic activity of mesoporous TiO2 aggregates by embedding carbon nanotubes as electron-transfer channel, Phys. Chem. Chem. Phys. 13 (2011). https://doi.org/10.1039/c0cp01139h.

[12] C.H. Huang, Y.M. Lin, I.K. Wang, C.M. Lu, Photocatalytic activity and characterization of carbon-modified titania for visible-light-active photodegradation of nitrogen oxides, Int. J. Photoenergy. 2012 (2012). https://doi.org/10.1155/2012/548647.

[13] Y.J. Xu, Y. Zhuang, X. Fu, New insight for enhanced photocatalytic activity of TiO2 by doping carbon nanotubes: A case study on degradation of benzene and methyl orange, J. Phys. Chem. C. 114 (2010). https://doi.org/10.1021/jp909855p.

[14] F. Liu, N. Feng, L. Yang, Q. Wang, J. Xu, F. Deng, Enhanced Photocatalytic Performance of Carbon-Coated TiO2- x with Surface-Active Carbon Species, J. Phys. Chem. C. 122 (2018). https://doi.org/10.1021/acs.jpcc.8b02716.

[15] H. Aliyeva, A. Gurel, S. Nowak, S. Lau, P. Decorse, S. Chaguetmi, D. Schaming, S. Ammar, Photo-anodes based on TiO2 and carbon dots for photo-electrocatalytical measurements, Mater. Lett. 250 (2019). https://doi.org/10.1016/j.matlet.2019.02.131.

[16] P.N.O. Gillespie, N. Martsinovich, Origin of Charge Trapping in TiO2/Reduced Graphene Oxide Photocatalytic Composites: Insights from Theory, ACS Appl. Mater. Interfaces. 11 (2019). https://doi.org/10.1021/acsami.9b09235.

[17] G. Žerjav, M.S. Arshad, P. Djinović, I. Junkar, J. Kovač, J. Zavašnik, A. Pintar, Improved electron-hole separation and migration in anatase TiO2 nanorod/reduced graphene oxide composites and their influence on photocatalytic performance, Nanoscale. 9 (2017). https://doi.org/10.1039/c7nr00704c.

[18] S. Charoenphon, A. Boonchun, D. Jarukanont, J. T-Thienprasert, P. Reunchan, Energetics and optical properties of carbon impurities in rutile TiO2, RSC Adv. 10 (2020). https://doi.org/10.1039/d0ra02709j.

[19] C. Di Valentin, G. Pacchioni, A. Selloni, Theory of carbon doping of titanium dioxide, Chem. Mater. 17 (2005). https://doi.org/10.1021/cm051921h.

[20] S. Huygh, A. Bogaerts, E.C. Neyts, How Oxygen Vacancies Activate CO2 Dissociation on TiO2 Anatase (001), J. Phys. Chem. C. 120 (2016). https://doi.org/10.1021/acs.jpcc.6b07459.

[21] M. Pierpaoli, A. Lewkowicz, M. Rycewicz, K. Szczodrowski, M.L. Ruello, R. Bogdanowicz, Enhanced photocatalytic activity of transparent carbon nanowall/TiO2 heterostructures, Mater. Lett. 262 (2020). https://doi.org/10.1016/j.matlet.2019.127155.

[22] Y. Xu, Y. Mo, J. Tian, P. Wang, H. Yu, J. Yu, The synergistic effect of graphitic N and pyrrolic N for the enhanced photocatalytic performance of nitrogen-doped graphene/TiO2 nanocomposites, Appl. Catal. B Environ. 181 (2016). https://doi.org/10.1016/j.apcatb.2015.08.049.

[23] Q. Li, B. Guo, J. Yu, J. Ran, B. Zhang, H. Yan, J.R. Gong, Highly efficient visible-light-driven photocatalytic hydrogen production of CdS-cluster-decorated graphene nanosheets, J. Am. Chem. Soc. 133 (2011). https://doi.org/10.1021/ja2025454.

[24] N.A.M. Noor, S.K. Kamarudin, M. Darus, N.F. Diyana, M. Yunos, M.A. Idris, Photocatalytic properties and graphene oxide additional effects in tio2, in: Solid State Phenom., 2018. https://doi.org/10.4028/www.scientific.net/SSP.280.65.

[25] M.M.J. Sadiq, U.S. Shenoy, D.K. Bhat, Enhanced photocatalytic performance of N-doped RGO-FeWO4/Fe3O4 ternary nanocomposite in environmental applications, Mater. Today Chem. 4 (2017). https://doi.org/10.1016/j.mtchem.2017.04.003.

[26] K. Natarajan, S. Dave, H.C. Bajaj, R.J. Tayade, Enhanced photocatalytic degradation of nitrobenzene using MWCNT/β-ZnMoO4 composites under UV light emitting diodes (LEDs), Mater. Today Chem. 17 (2020). https://doi.org/10.1016/j.mtchem.2020.100331.

[27] P. Boldrin, E. Ruiz-Trejo, J. Mermelstein, J.M. Bermúdez Menéndez, T. RamÍrez Reina, N.P. Brandon, Strategies for Carbon and Sulfur Tolerant Solid Oxide Fuel Cell Materials, Incorporating Lessons from Heterogeneous Catalysis, Chem. Rev. 116 (2016). https://doi.org/10.1021/acs.chemrev.6b00284.

[28] T. Ohno, T. Tsubota, K. Nishijima, Z. Miyamoto, Degradation of methylene blue on carbonate species-doped TiO2 photocatalysts under visible light, Chem. Lett. 33 (2004). https://doi.org/10.1246/cl.2004.750.

[29] X. Li, J. Xiong, Y. Xu, Z. Feng, J. Huang, Defect-assisted surface modification enhances the visible light photocatalytic performance of g-C3N4@C-TiO2 direct Z-scheme heterojunctions, Cuihua Xuebao/Chinese J. Catal. 40 (2019). https://doi.org/10.1016/S1872-2067(18)63183-3.

[30] J. Gamage McEvoy, W. Cui, Z. Zhang, Degradative and disinfective properties of carbon-doped anatase-rutile TiO2 mixtures under visible light irradiation, in: Catal. Today, 2013. https://doi.org/10.1016/j.cattod.2012.04.015.

[31] X. Fan, T. Wang, Y. Guo, H. Gong, H. Xue, H. Guo, B. Gao, J. He, Synthesis of ordered mesoporous TiO2-Carbon-CNTs nanocomposite and its efficient photoelectrocatalytic methanol oxidation performance, Microporous Mesoporous Mater. 240 (2017). https://doi.org/10.1016/j.micromeso.2016.10.049.

[32] M. Ouzzine, A.J. Romero-Anaya, M.A. Lillo-Ródenas, A. Linares-Solano, Spherical activated carbon as an enhanced support for TiO2/AC photocatalysts, Carbon N. Y. 67 (2014). https://doi.org/10.1016/j.carbon.2013.09.069.

[33] K. Woo, W.I. Lee, J.S. Lee, S.O. Kang, Novel titanium compounds for metal-organic chemical vapor deposition of titanium dioxide films with an ultrahigh deposition rate, Inorg. Chem. 42 (2003). https://doi.org/10.1021/ic0256967.

[34] G. Fu, P. Zhou, M. Zhao, W. Zhu, S. Yan, T. Yu, Z. Zou, Carbon coating stabilized Ti3+-doped TiO2 for photocatalytic hydrogen generation under visible light irradiation, Dalt. Trans. 44 (2015). https://doi.org/10.1039/c5dt01204j.

[35] L.H. Yu, C.H. Kuo, C.T. Yeh, Poly(vinylpyrrolidone)-modified graphite carbon nanofibers as promising supports for PtRu catalysts in direct methanol fuel cells, J. Am. Chem. Soc. 129 (2007). https://doi.org/10.1021/ja072367a.

[36] Y.C. Sharma, Adsorption characteristics of a low-cost activated carbon for the reclamation of colored effluents containing malachite green, J. Chem. Eng. Data. 56 (2011). https://doi.org/10.1021/je1008922.

[37] J. Wang, R. Ran, M.O. Tade, Z. Shao, Self-assembled mesoporous TiO2/carbon nanotube composite with a three-dimensional conducting nanonetwork as a high-rate anode material for lithium-ion battery, J. Power Sources. 254 (2014). https://doi.org/10.1016/j.jpowsour.2013.12.090.

[38] L. Yu, Y. Lin, J. Huang, S. Lin, D. Li, A Visible Light Photocatalyst of Carbonate-Like Species Doped TiO2, J. Am. Ceram. Soc. 100 (2017). https://doi.org/10.1111/jace.14552.

[39] H. Yang, L. Zhai, K. Li, X. Liu, B. Deng, W. Xu, A highly efficient nano-graphite-doped TiO2 photocatalyst with a unique sea-island structure for visible-light degradation, Catal. Sci. Technol. 10 (2020). https://doi.org/10.1039/c9cy02179e.

[40] P. Wang, Q. Zhou, Y. Xia, S. Zhan, Y. Li, Understanding the charge separation and transfer in mesoporous carbonate-doped phase-junction TiO2 nanotubes for photocatalytic hydrogen production, Appl. Catal. B Environ. 225 (2018). https://doi.org/10.1016/j.apcatb.2017.11.069.

[41] M. Sharma, M. Poddar, Y. Gupta, S. Nigam, D.K. Avasthi, R. Adelung, R. Abolhassani, J. Fiutowski, M. Joshi, Y.K. Mishra, Solar light assisted degradation of dyes and adsorption of heavy metal ions from water by CuO–ZnO tetrapodal hybrid nanocomposite, Mater. Today Chem. 17 (2020). https://doi.org/10.1016/j.mtchem.2020.100336.

[42] K. Sayama, H. Arakawa, Effect of carbonate addition on the photocatalytic decomposition of liquid water over a ZrO2 catalyst, J. Photochem. Photobiol. A Chem. 94 (1996). https://doi.org/10.1016/1010-6030(95)04204-0.

[43] N.M. Dimitrijevic, B.K. Vijayan, O.G. Poluektov, T. Rajh, K.A. Gray, H. He, P. Zapol, Role of water and carbonates in photocatalytic transformation of CO 2 to CH4 on titania, J. Am. Chem. Soc. 133 (2011). https://doi.org/10.1021/ja108791u.

[44] M.K. Nowotny, T. Bak, J. Nowotny, Electrical properties and defect chemistry of TiO2 single crystal. IV. Prolonged oxidation kinetics and chemical diffusion, J. Phys. Chem. B. 110 (2006). https://doi.org/10.1021/jp060624c.

[45] M.K. Nowotny, T. Bak, J. Nowotny, Electrical properties and defect chemistry of TiO2 single crystal. III. Equilibration kinetics and chemical diffusion, J. Phys. Chem. B. 110 (2006). https://doi.org/10.1021/jp060623k.